A R C H I V E S O F M E T A L L U R G Y A N D M A T E R I A L S
Volume 59 2014 Issue 1
DOI: 10.2478/amm-2014-0064

B. RAMS*, A. PIETRAS*, K. MROCZKA**

# FRICTION STIR WELDING OF ELEMENTS MADE OF CAST ALUMINIUM ALLOYS

# ZGRZEWANIE METODĄ FSW ELEMENTÓW WYKONANYCH Z ODLEWNICZYCH STOPÓW ALUMINIUM

The article presents application of FSW method for joining elements made of cast aluminium alloys which are hardly weldable with other known welding techniques. Research's results of plasticizing process of aluminium and moulding of seam weld during different FSW process' conditions were also presented. Influence of welding parameters, shape and dimensions of tool on weld structure, welding stability and quality was examined. Application of FSW method was exemplified on welding of hemispheres for valves made of cast aluminium alloy EN AC-43200.

*Keywords*: Friction Welding, FSW, butt welding, cast aluminium alloy

W artykule przedstawiono zastosowanie metody FSW do łączenia elementów z trudno spajanego znanymi technikami spawalniczymi aluminium odlewniczego. Przedstawiono również wyniki badania procesu uplastyczniania aluminium oraz formowania się zgrzeiny liniowej w różnych warunkach prowadzenia procesu zgrzewania FSW. Badano wpływ parametrów procesu zgrzewania oraz kształt i wymiary narzędzia na strukturę zgrzein oraz na stabilność i jakość zgrzewania. Zastosowanie metody zgrzewania FSW przedstawiono na przykładzie łączenia czasz kul zaworów wykonanych z odlewniczego stopu aluminium EN AC-43200.

## 1. Introduction

FSW (Friction Stir Welding) is the method that makes it possible to successfully join aluminium and its alloys, including casting alloys which are difficult to weld using known welding techniques. This method is increasingly used in the world mainly in the shipbuilding, rail, automotive and building industries.

In FSW process the stirring and rotating tool penetrating material along the line of welding is applied for the friction heating and softening material. After the tool is put into rotation and frictional heating and softening the material around the probe, the tool is traversed along the joint line. The heated and plasticised materials of the components being welded are extruded around the tool probe backwards, where before cooling down they are stirred and upset by the shoulder. In the centre of the weld the zone called "nugget" is formed in the result of the stirring of the softened metals of both parts being welded behind the tool [1,2].

The shape and dimensions of the weld depend on the shape and size of the stirring tool and applied welding parameters.

Basic parameters of FSW process comprise: tool rotation speed, $V_n$[rpm]; welding speed, $V_{zg}$[mm/min]; tilt angle, $\alpha$ [°]; tool type and size of the tool: probe diameter – d [mm], shoulder diameter – D [mm], probe length – l [mm].

During FSW process material of the workpiece is subjected to mechanical stirring and intensive plastic deformation at higher temperature, which spreads out also outside the stirring zone (thermo mechanical affected zone). Additionally, the significant temperature gradient occurs across the weld outside the thermo mechanical affected zone (heat affected zone). As the result of those factors more complex structure is being formed in the cross-section of the weld, which influences directly its mechanical properties [4-7]. In case of aluminium casting alloys welding, the changes in the microstructure are associated both with processes of deforming, recovery and recrystallization and also with microstructure component phase changes, e.g. with precipitation or dissolving of intermetallic phases [8]. There is a tendency to produce a weld free from flaws which can occur in conventional arc welding methods.

The aim of this research was finding the relation between welding conditions – welding parameters and a tool shape – on a weld structure and the stability and quality of welding.

## 2. Research station

The investigation into FSW process was conducted at Instytut Spawalnictwa on the vertical milling machine FYF32JU2 equipped with special clamps fixing the welded parts. The station for testing of linear welding of plates is

* INSTYTUT SPAWALNICTWA W GLIWICACH, ZAKŁAD TECHNOLOGII ZGRZEWANIA I INŻYNIERII ŚRODOWISKA, POLAND
** UNIWERSYTET PEDAGOGICZNY W KRAKOWIE, INSTYTUT TECHNIKI, POLAND

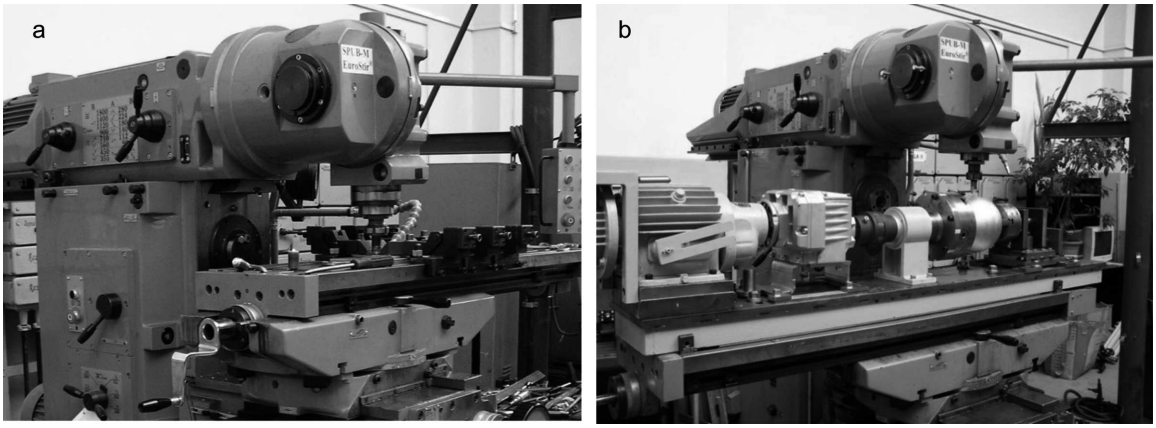


Fig. 1. Station for FSW welding process, a) tooling for plate welding, b) tooling for valve balls welding

TABLE 1

Chemical composition of the EN AC-43200 aluminium alloy [3]

| Alloy denotation | | Elements content, [%] | | | | | | | | |
|---|---|---|---|---|---|---|---|---|---|---|
| numerical | chemical symbol | Si | Cu | Mg | Mn | Fe | Ti | Zn | Ni | Al |
| EN AC-43200 | EN AC-Al Si10Mg(Cu) | 9.00-11.00 | 0.35 | 0.20-0.45 | 0.55 | 0.65 | 0.20 | 0.35 | 0.15 | rest |

shown in Fig. 1a and Fig. 1b presents the station for welding of balls, equipped with a special positioner.

Three tool types of a shoulder diameter of 20 mm were used during the research: cone probe (l = 4.0 mm), conventional probe (l = 5.8 mm) and Triflute probe (l = 5.8 mm). Additionally the tool without a probe was used (D=15 mm and D=18 mm). The tool tilt angle was 1.5°. The shapes of the tools used in research are shown in Fig. 2.

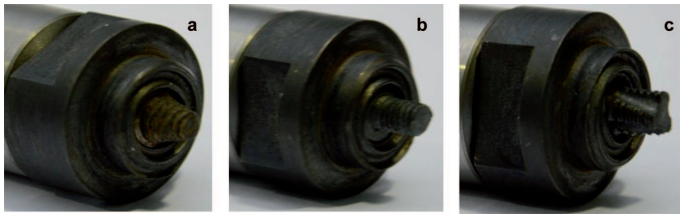


Fig. 2. Stirring tools used during research into FSW process a) cone probe, b) conventional probe, c) Triflute probe

## Tested material

In quality testing of FSW process 6.0 mm thick plates and components of ball parts made of aluminium alloy EN AC-43200 were used. Chemical composition of the EN AC-43200 alloy is shown in Table 1.

## Testing of FSW butt welding with a tool without a probe

During testing the possibility of producing butt weld in 6.0 mm thick plates of aluminium casting alloy EN AC 43200 was investigated. The testing of the structure quality of a weld was performed using a tool without a probe and of a shoulder diameter D = 18 mm ($\alpha$ =1.5°) and welding parameters as in Table 2. The example of this weld structure is shown in Fig. 3.

TABLE 2

Welding parameters

| No. | Tool type | Parameters of tool motion | |
|---|---|---|---|
| | | $V_n$ [rpm] | $V_{zg}$[mm/min] |
| 1 | Shoulder ø 18 mm, without a probe | 560 | 224 |
| 2 | | 560 | 180 |
| 3 | | 450 | 224 |
| 4 | | 450 | 180 |

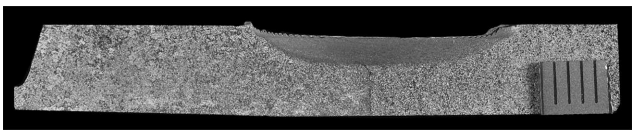

Fig. 3. FSW weld structure. Welding parameters: no. 4 of Table. 2

## Testing of conventional FSW butt welding process

Butt welding of cast plates of EN AC 43200 alloy, 6.0 mm thick, was conducted for parameters as in Table 3, using conventional and Triflut tools ($\alpha$ =1.5°). Below in Fig 4-5 the examples of weld structures obtained during microscopic examination are shown. The welds were characterised by compact structures without flaws and discontinuities visible in macroscale. In photographs the advancing side is on the right.

TABLE 3

Welding parameters

| No. | Tool type | Parameters of tool motion | |
|---|---|---|---|
| | | $V_n$ [rpm] | $V_{zg}$ [mm/min] |
| 1 | Conventional | 560 | 280 |
| 2 | Conventional | 710 | 355 |
| 3 | Triflute | 710 | 355 |

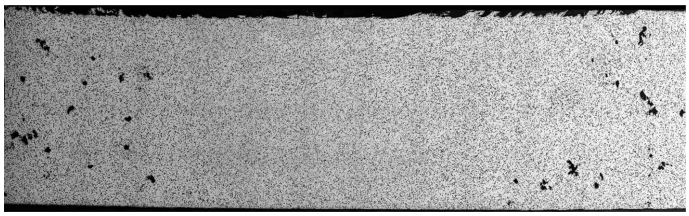

Fig. 4. FSW weld structure. Welding parameters: no. 1 of Table 3

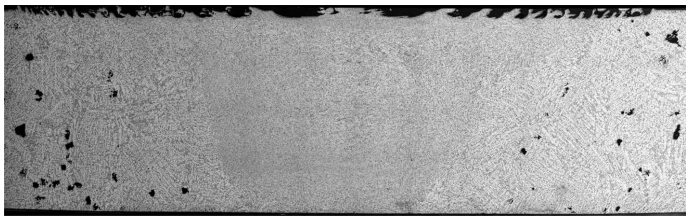

Fig. 5. FSW weld structure. Welding parameters: no. 3 of Table 3

The tool with 5.8 mm long probe made it possible to produce welds of the proper structure in the whole thickness in plates of 6.0 mm thick. The whole joints are illustrated in Fig. 4-5. The selected areas of joints are presented in Fig. 6-10.

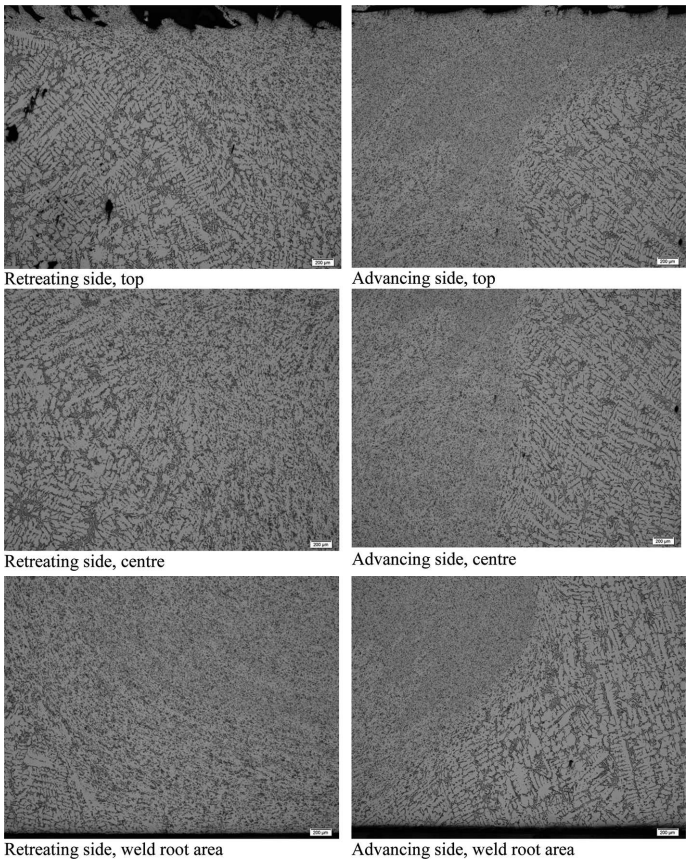


Fig. 6. Separate areas of a weld from Fig. 4. Welding parameters: no. 1 of Table 3

The area subjected to the significant strains and deformations was tested from the viewpoint of the alloying elements content. Mainly particles containing Fe were tested, what made it possible to equivocally distinguish them from Si eutectic precipitations, which are of predominant character. The examples of observations, made using SEM microscopy in BEC mode of observation and EDS analysis are shown in Fig. 11-12. In Fig. 12 b the structure of parent material including particles of $Al_3(FeMn)$ phase distributed in the skeleton form, which after welding process undergo fragmentation and deformation (Fig. 12a). The occurrence of these particles in the form of short bands indicates their local segregation.

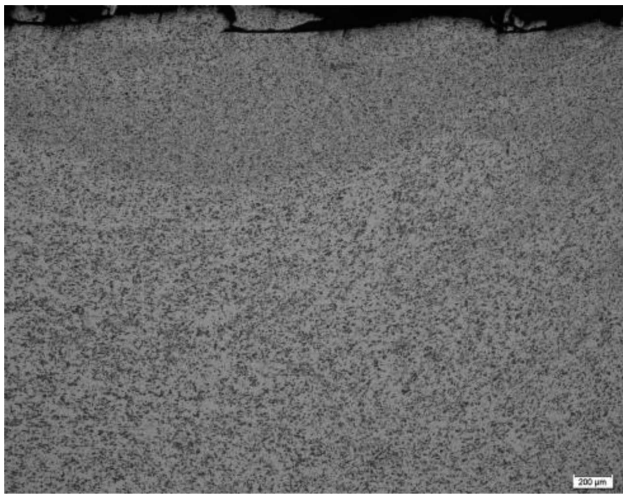


Fig. 7. A fragment of the weld from the area close to the surface in the center

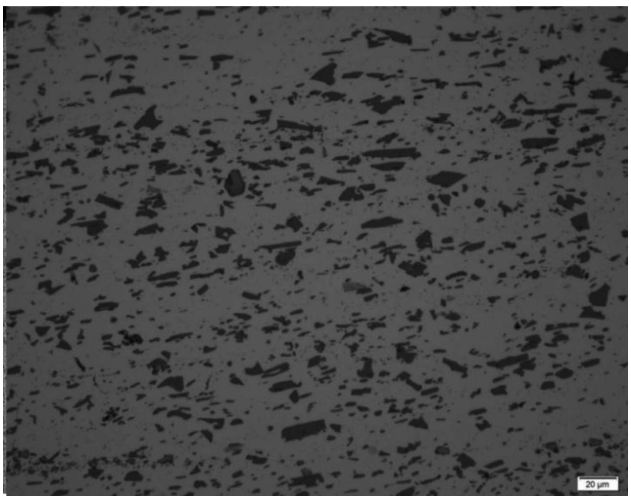


Fig. 8. An image of the weld under the face in the central area

The calculations of the average size of the particle and shape factor for parent material were performed. The same calculations were conducted for the area located in the weld axis, in the distance of 1 mm from weld face. Microstructure of this region is shown in Fig. 7. The calculations have revealed that medium parent material particle size is 80.2 $\mu m^2$, with standard deviation of 107.4, whereas average shape factor is 0.34, with standard deviation 0.23. In Fig. 13 and 14 histograms of the particles occurrence frequency in separate intervals of shape factor are presented. In parent material (Fig. 13) very elongated particles dominate – 12.8% particles have shape factor below 0.1, and 54% particles below 0.3. For the tested area of a weld (Fig. 14) only 13.5% particles have the shape factor below 0.3, whereas the particles of shape factor between 0.3 do 0.8 are the dominant (68.4%). The research results have indicated that plastic deformation occurring while

welding caused very high refinement of particles and changed their shape towards particles being more equiaxial.

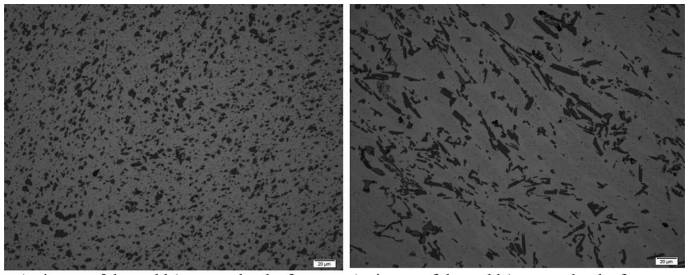

An image of the weld 1 mm under the face from retreating side

An image of the weld 1 mm under the face from advancing side

Fig. 9. An image of the weld from retreating and advancing side

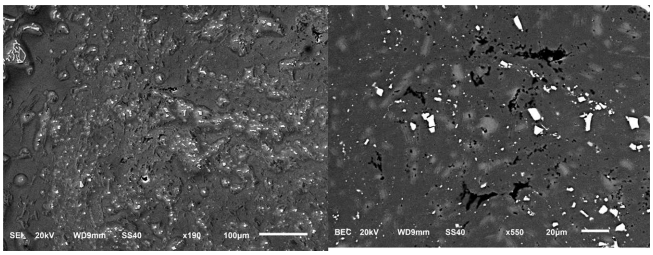

Fig. 10. Microflaws in a weld. Central part of a weld (SEM)

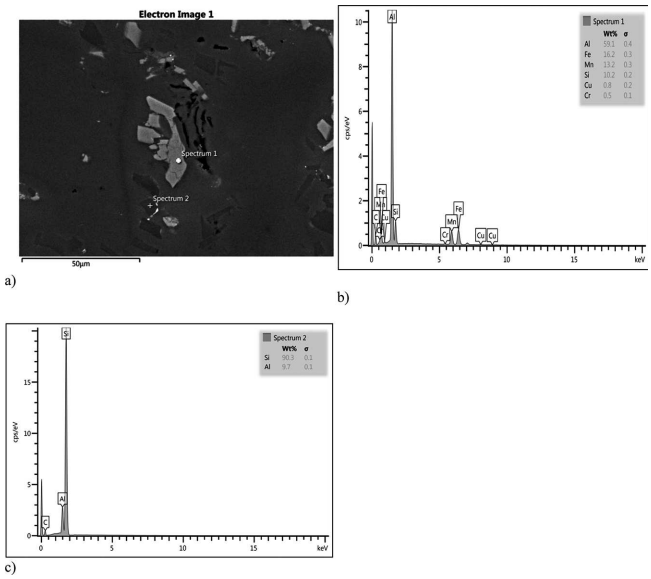


Fig. 11. A fragment of a sample welded at parameters no. 3 – a). Distribution of elements (EDS analysis) in the selected points; in the point: 1 – b), in the point 2 – c)

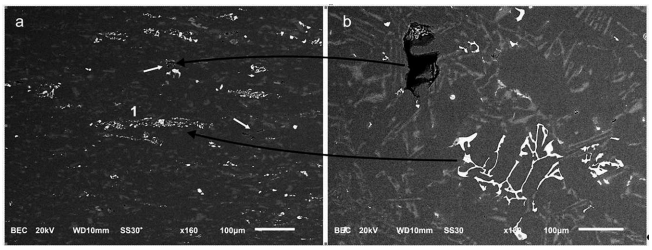


Fig. 12. Flaws in parent material and structures of casting alloy – b) as well as broken and mixed during FSW process – a). Parameters: no. 2 of Table 3 (SEM)

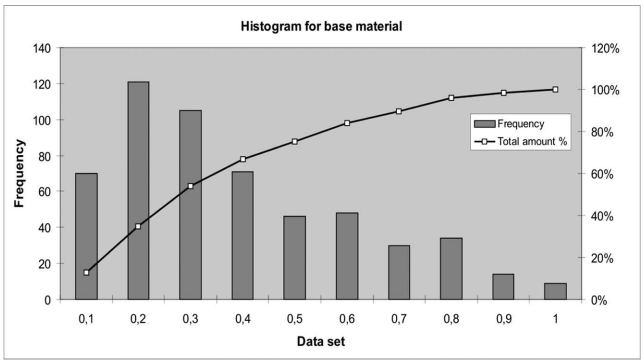


Fig. 13. The measurement of grain size in parent material of casting alloy. Parameters no. 2 of Table 3

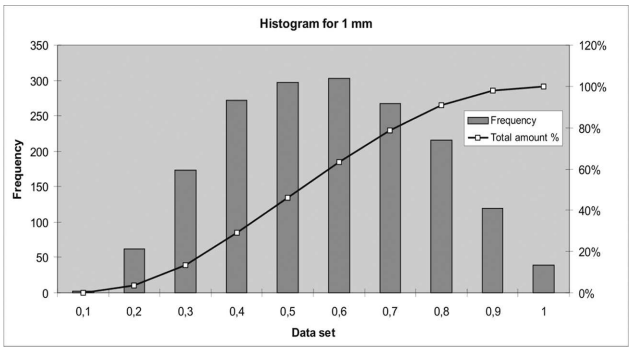


Fig. 14. The measurement of grain size in material of central part of a weld. Parameters no. 2 of Table 3

The samples were subjected to hardness measurements along the measuring line on the depth of 1 and 4 mm under the weld face directly after welding, after natural and artificial aging, as well as after solutioning and aging. Parameters of heat treatment are as follows: temperature of solutioning: 530°C/30 min, cooling in water, and temperature of aging: 180°C/20 hours. Overall results of the average hardness measurements in the cross-section of a weld conducted along the measuring line, 1 mm under the weld face are shown in the diagram – Fig. 15.

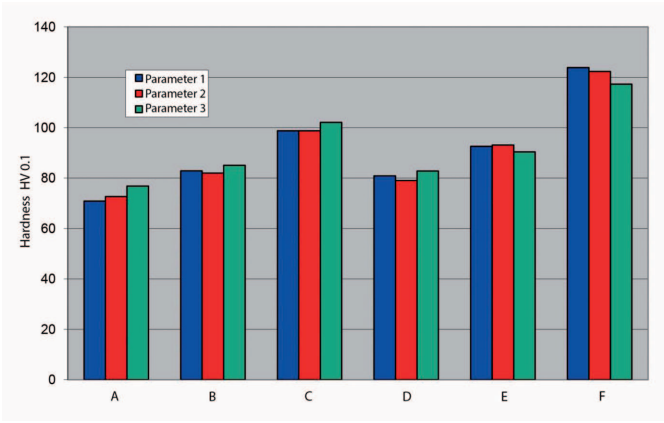


Fig. 15. A comparison of average hardness measurements in the cross-section of a weld conducted along the measuring line, 1 mm under the weld face. Parameters: no. 1, 2, 3 of Table 3. A – after welding, B – after welding and natural aging, C – after welding and artificial aging, D – after solutioning, E – after solutioning and natural aging, F – after solutioning and artificial aging

### Testing of the process of welding valve balls parts

Basing on the research results the FSW process was selected for joining valve ball parts made of aluminium casting alloy EN AC-43200. Ball parts of a diameter of 110 mm (wall thickness 10 mm) were welded using a tool of a shoulder diameter D=15 mm, without a probe and with cone probe (l=4.0mm). Welding parameters applied during testing of balls welding are shown in Table 4.

TABLE 4
Welding parameters applied in testing of welding the ball of EN AC-43200

| No. | Tool type | Parameters of tool motion | |
|---|---|---|---|
| | | $V_n$ [rpm] | $V_{zg}$ [mm/min] |
| 1 | Shoulder ø 15 mm, without a probe | 710 | 345 |
| 2 | | 710 | 690 |
| 3 | Cone tool | 710 | 560 |
| 4 | | 710 | 690 |
| 5 | | 900 | 1030 |

During research the process of weld face forming and weld structure were analysed. Research has revealed that from the viewpoint of weld strength there is no need to plasticise metal in the whole thickness of welded workpieces. The permanent joint was successfully produced with a tool penetrating welded material only on the certain depth. The quality of welding using a tool without a probe was also tested, when the depth of a tool interaction is relatively small.

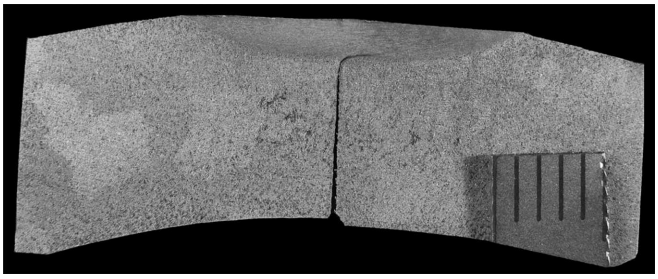

Fig. 16. FSW weld structure. Welding using a tool without a probe. Welding parameters: no. 1 of Table 4

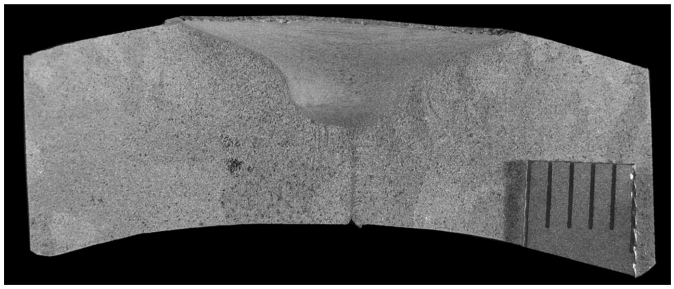

Fig. 17. FSW weld structure. Welding using a cone tool. Welding parameters: no. 4 of Table 4

The strength of welded balls was tested in the pressure test. In the result of this test it has been found that all balls welded using a tool without a probe were destroyed at the test pressure exceeding 80 bars. Balls welded with the tool with a cone probe were destroyed by fracture in the thermo mechanical affected zone (or in the boundary of this zone and HAZ) at pressure of over 150 bars.

The examples of tested welds structures of the balls are shown in Fig. 16 (welded without a probe) and Fig. 17 (welded with a cone tool). The macrostructure of a weld is shown in Fig. 18. Fig. 19-20 present fragments of a weld structure of a joint from Fig. 18.

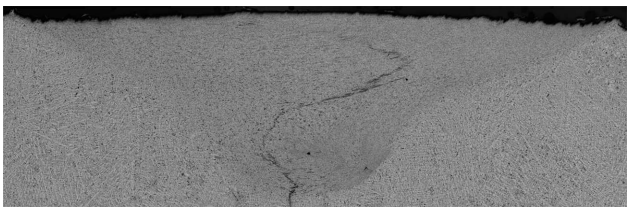

Fig. 18. FSW weld structure. Welding parameters: no. 3 of Table 4

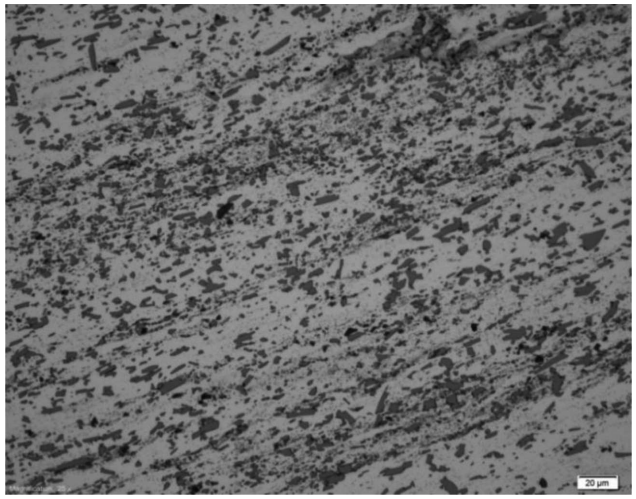

Fig. 19. Fragment of Fig. 18 – central area of a weld with visible layer of not broken oxides near a weld „nugget"

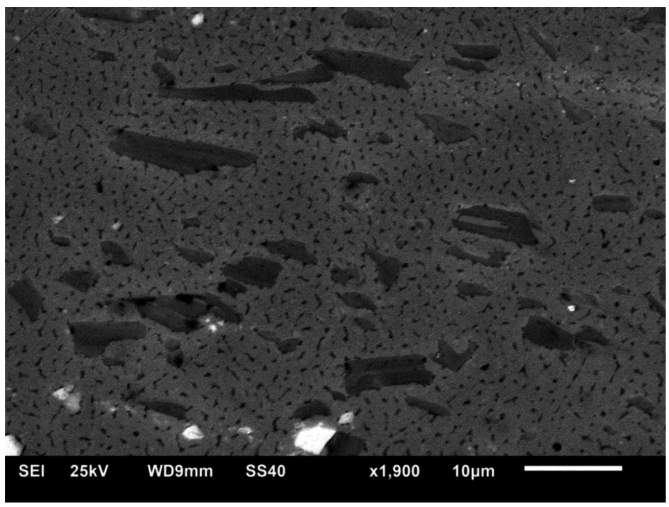


Fig. 20. Fragment of the Fig. 18. SEM analysis. Strong refinement of the weld nugget structure

## Summary

The conducted tests made it possible to determine the influence of the tools on the process of friction weld forming during butt welding of casting aluminium plates. The plates were butt welded using a tool without a probe, conventional tool and a tool of Triflute type.

Testing with a tool without a probe has revealed that at low welding speed it is possible to obtain welds of compact structure but the depth is small. For some applications such weld thickness is sufficient. For instance the strength of the ball welded in such a way and obtained in pressure test has revealed that the failure of the ball is caused only when the pressure was higher than 80 bar.

A weld formed correctly and of the adequate dimensions and load capacity is produced while welding with a tool with a probe. Testing of a structure of butt joints in casting alloys has revealed that the weld quality is higher of that of parent material. Casting material contains higher or lower agglomerations of micro-shrinkages and discontinuities. During friction welding many of these imperfections are eliminated. There are however micro-shrinkages in material of such a big dimensions that even intensive thermal-plastic processing of material during FSW process fails to eliminate them.

Macroscopic structure of a weld is well visible as the material structure in the zone of thermo mechanical plasticisation undergoes transformation in the result of plastic strain occurring with large degree of deformation. This zone is not homogeneous. Basing on the particles distribution it is possible to determine the position of the so called weld nugget – central region in Fig. 6-8. The area covers approximately 30% of the whole zone of material thermal-plastic deformation. Like in the typical FSW welds, the advancing side is characterised by the distinctly marked boundary between the plastically deformed zone and heat affected zone (HAZ).

Weld microstructure testing has revealed that basing on the distribution and size of particles it is possible to find that this boundary is the transition zone between material not plastically deformed and an area of strong deformation. In the transition zone Si particles are mechanically fragmented (broken) but their distribution still remains the microstructure of cast material. The grains of the metallic matrix in this region are elongated accordingly to the direction of material transferring while welding and fail to undergo the processes of structure renewal – recrystallization or recovery with the participation of subgrains coalescence process. The transition zone on the other side of a weld, i.e. on retreating side, is considerably wider what results in the less distinct boundary with HAZ material. Macrostructure analysis shows that the reaction of a shoulder on its edges has limited influence on the weld structure. The region of material deformation under the weld face surface occurs on the depth bigger than 1 mm only in the distance of about 7.8 mm from weld axis. As the probe radius is relatively small (4 mm) the contact of material with a shoulder is in the distance of 9 mm, and the range of shoulder interaction, as above, is 3.8 mm, which is about 42%. Such a result implies that from the viewpoint of its reaction on the weld structure, the diameter of a shoulder can be smaller than that used currently.

In case of properly produced weld, in the joint cross-section there are no visible imperfections in all regions of a joint. It is also possible to avoid the frequently occurring kissingbond defect.

One of the characteristic features of the majority of FSW joints is the considerable diversification of the microstructure. In the separate regions of a weld the material is subjected to the thermal-plastic treatment of various degrees. This concerns the degree of the deformation, temperature of the deformation process as well as the distance of the material transport resulting from the tool motion. On the basis of the comparison of the particles size in parent and weld joint materials it is possible to determine the degree of the material refinement. Welds in casting alloys are excellent for such analysis as precipitations, mainly Si, in the cast are of significant sizes and their shapes are elongated in the majority of cases. Thanks to this structure feature it was possible to perform the calculations of the average particle size and the size factor for parent metal and for the area located in the joint axis, in the distance of 1 mm from the weld face. The calculated average parent material particle size, of the average size factor 0.34, is 80.2 $\mu m^2$. In turn the average particle size in the analysed joint area (1 mm from the face, centre) is 12.4 $\mu m^2$. This means that the plastic deformation in this region caused 6-fold refinement of the particles. The fragmentation of the particles simultaneously caused their shortening and changed the shape into more oval one.

Macroscopic and microscopic analysis indicates the inhomogeneity of the particles distribution in the separate microregions. The areas in the direct vicinity of the weld face reveal the substantial unification of the distribution in contrast with the regions located closer to the weld nugget. The particles banding resulting from the direction of the material flow can also be observed.

The testing of the welding region focused on the particles containing Fe allowed for their unequivocal distinguishing from the dominant, eutectic Si precipitations. The particles containing Fe, Mn, Al (it is probably phase $Al_3(FeMn)$), are arranged in short bands – the example of a band is marked as no. 1 in Fig. 12a. Such an arrangement of the particles in the microstructure indicates their local segregation. The reasons for this segregation beyond any doubt are not associated with the processes of diffusion and precipitation, and should be looked for in the way of plasticisation and displacement in the tested region. Testing of the parent material has revealed the presence of the phase of the chemical composition analogical to that which occurs locally in the form of the skeleton structures. The example of this precipitation is shown in Fig. 12b (SEM-BEC observation). Chemical composition in both cases (in parent material and in the joint) was analysed using SEM-EDS method. Such a result of the observation makes it possible to conclude that material in the region above the weld nugget is subjected to the significant stresses and plastic flow, what causes particle fragmentation without the creation of a mixture. For this reasons the skeleton structure of the phase with Fe content being present in the parent material has been broken and transformed into the particles band visible in the joint region being discussed (Fig. 12a). This conclusion also brings the explanation of the presence of micro-flaws in the tested area. The examples of imperfections are marked with

arrows in Fig. 12. Their origin is associated with the presence of casting defects, so-called shrinkage porosity in parent material. During welding process these flaws will behave like phases occurring locally. When material is not being mixed they will only be deformed. State of stresses in the analysed part of the joint and the range of material flow occurred to be insufficient for the elimination (so-called recovery) of those imperfections. Their size however became significantly smaller. The imperfections in parent material, which sizes were smaller, were eliminated by upsetting.

Testing of mechanical properties of butt welds produced in cast plates were confined to the determination of the hardness distribution. Hardness measurements were conducted in the distance of 1 and 4 mm from the weld face of three samples produced at various welding parameters. Tests were performed for weld testpieces being in three states: after welding, after the natural aging and after the artificial aging. The acquired results make it possible to conclude that the microstructure directly after welding is in the metastable state and over time or as a result of the heat treatment undergoes changing, which causes hardening of material. This conclusion is confirmed also by the results of the average hardness calculations performed on the basis of the separate hardness distributions. The average hardness of the weld in the state after welding was 73 HV0.1, after natural aging 82 HV0.1 and after artificial aging 99 HV0.1.

The process of natural aging causes distinct increase in material hardness in the distance of –5 to +5 mm from the welding line, thus in the range of tool probe action. In the remaining regions, in this case in the heat affected zone, the material hardness is similar to that of material being in the state after welding and gradually increases with the distance from the welding line. The highest material hardness in the tested region was found for the joint after heat treatment, i.e. the artificial aging. The increase in hardness can be observed in the whole joint, and especially in the zone plastically deformed, where the value of about 107 HV0.1 was noticed, i.e. by 37HV higher comparing to the state after welding. Probably regardless of the distance from the weld face, material after welding will be hardening in the aging processes and the hardness increase reaches approximately 20% after natural aging and approximately 30% as a result of the artificial aging. The degree of material hardening depends on the place in the joint – the region being plastically processed is more susceptible to aging processes than heat affected zone.

Microstructure of the correct weld obtained during welding of ball parts reveals the same features and characteristic structures as that observed in the cross sections in butt welds. The structure of a weld is continuous and contains correctly formed weld nugget. By design the ball parts were not welded through the whole thickness of 10 mm, but only to the depth of 6 mm that was associated with the length of a tool probe. Therefore in the cross sections the oxides band is visible clearly, which is distributed in zigzag characteristic for FSW joints [5]. Such oxide inclusions do not reduce the joint strength.

## Conclusions

On the basis of the research result analysis carried out at Instytut Spawalnictwa the following conclusions were drawn:

- FSW process can be applied for joining components of casting aluminium. Correctly selected welding parameters make it possible to obtain good quality joints – without macro and microscopic imperfections and of the required mechanical properties.
- In the region between the face and weld nugget the material is strongly deformed, what causes the refinement of the particles, however simultaneously material is not mixed.
- In the FSW joint of casting material containing imperfections, so called shrinkage porosity, submicron discontinuities of the microstructure can occur in the regions where material is not mixed enough – e.g. in the area between the face and weld nugget or in the zones boundary. In these regions the plastic distortion may fail to provide the full elimination of such discontinuities.
- Plastic strain caused by a tool shoulder (under the face surface) depends on welding parameters and a tool size and is very limited in the regions being more distant from the tool axis.
- During FSW process the microstructure of hypoeutectic silumin in the regions close to weld face undergoes significant refinement due to mechanical fragmentation of the particles. The particles shape factor is also changing towards more equiaxial one.
- Material of FSW joint, made in components of casting alloy, directly after the welding process is in the metastable state. As the result of both natural and artificial aging, the material in the weld regions undergoes hardening. The process of the artificial aging is more effective and significantly influences the hardening of material of the joint.

### Acknowledgements

The article contains the selected research results obtained in the project conducted within INNOTECH programme and entitled ”Production of bimetallic components using advanced techniques of friction welding process” INNOTECH-K1/IN1/28/150092/NCBR/12, 2012-2015.

REFERENCES

[1] W.M. T h o m a s, Friction Stir Butt Welding. Int. Patent Application. PCT/GB92/02203.1991

[2] K. M r o c z k a, J. D u t k i e w i c z, A. P i e t r a s, Characterization of friction stir welds of 6013 and 6013/2017A aluminium alloy sheets. Inżynieria Materiałowa **30**, 3 (2010).

[3] PN-EN 1706:2010. Aluminium i stopy aluminium – Odlewy – Skład chemiczny i własności mechaniczne.

[4] K. K r a s n o w s k i, P. S ę d e k, M. Ł o m o z i k, A. P i e t r a s, Impact of selected FSW parameters on mechanical properties of 6082-T6 aluminium alloy butt joints. Archives of Metallurgy and Materials **56**, 2011.

[5] H. O k a m u r a, K. A o t a, M. S a k a m o t o, Behaviour of oxides during friction stir welding of aluminium alloy and their effect on its mechanical properties. Welding International 4, 2002.

[6] Y. M a t s u, K. O k a p i, Y. T a m a k i, Fatigue behaviour of dissimilar friction stir welds between cast and wrought aluminium alloys. Strength of Materials **40**, 1 (2008).
[7] M.S. W ę g l o w s k i, A. P i e t r a s, A. W ę g l o w s k a, Effect of welding parameters on mechanical and microstructural properties of Al 2024 joints produced by friction stir welding. Journal of Kones Powertrain and Transport **19**, 1 (2009).
[8] G. L u a n, G. L i, W. W a n g, Ju K a n g, The Fundamental Research of the Friction Flow Welding. The 8th International Friction Stir Welding Symposium, Germany, 18-20 May 2010.

*Received: 10 May 2013.*